


12-2017

Cost-Savings of Implementing Site-Specific Ground Motion Response Analysis in Design of Mississippi Embayment Bridges

Ethan Ryan Benton Baker
University of Arkansas, Fayetteville

Follow this and additional works at: <http://scholarworks.uark.edu/etd>

 Part of the [Civil Engineering Commons](#), and the [Geotechnical Engineering Commons](#)

Recommended Citation

Baker, Ethan Ryan Benton, "Cost-Savings of Implementing Site-Specific Ground Motion Response Analysis in Design of Mississippi Embayment Bridges" (2017). *Theses and Dissertations*. 2572.
<http://scholarworks.uark.edu/etd/2572>

This Thesis is brought to you for free and open access by ScholarWorks@UARK. It has been accepted for inclusion in Theses and Dissertations by an authorized administrator of ScholarWorks@UARK. For more information, please contact scholar@uark.edu, ccmiddle@uark.edu.

Cost-Savings of Implementing Site-Specific Ground Motion Response Analysis in Design of
Mississippi Embayment Bridges

A thesis submitted in partial fulfillment
of the requirements for the degree of
Master of Science in Civil Engineering

by

Ethan Baker
University of Mississippi
Bachelor of Science in Civil Engineering, 2016

December 2017
University of Arkansas

This thesis is approved for recommendation to the Graduate Council.

Clinton Wood, Ph.D.
Thesis Director

Eric Fernstrom, Ph.D.
Committee Member

Gary Prinz, Ph.D.
Committee Member

Abstract

Deep dynamic site characterization and a site-specific ground motion response analysis (SSGMRA) were conducted for a bridge site in Monette, Arkansas. The SSGMRA indicated the design acceleration response spectrum determined using the American Association of State Highway and Transportation Officials (AASHTO) general seismic procedure could be reduced by 1/3 for the short period range due to attenuation of the short-period ground motions. The steel girder pile-bent bridge, originally designed using the AASHTO general seismic design procedure, was redesigned using the updated seismic demands estimated from SSGMRA. A cost-savings analysis was then conducted to determine the potential savings associated with conducting the SSGMRA. By designing based on the results of the SSGMRA, a potential savings of \$205,000 or 7% of the original bridge construction cost could be achieved for the study bridge. Items that contributed most to the cost savings were the pile and embankment construction.

©2017 by Ethan Baker
All Rights Reserved

Acknowledgements

I would like to sincerely thank Dr. Clinton Wood. His guidance has helped me to gain great knowledge in a field I knew very little about two years ago. His work ethic is unmatched, and I have become a better engineer by attempting to emulate it. I am truly thankful for the opportunity to work with him and even more thankful to call him my friend.

I would also like to thank Dr. Eric Fernstrom and Dr. Gary Prinz for serving as members of my thesis committee. I am also thankful for Steve Peyton, Courtney Rome, and Matt Green who gave me guidance throughout this research project. I would like to acknowledge the support of this project from the Arkansas Department of Transportation. I would like to thank our Geotechnical Earthquake Engineering lab team for help with the field testing and data processing for this project. Lastly, I would like to thank the farmers of Northeast Arkansas who allowed us to take surface wave measurements in between their rows of crops during their busiest of seasons.

Dedication

This thesis is dedicated to my family. My parents, Ryan and Christy Baker, as well as my sister Morgan Ransone, have supported and believed in me my entire life. My wife, Olivia Baker, has been there for me throughout my entire graduate career. Without these people, I would not be the man I am today.

Table of Contents

1. Introduction	1
2. Monette, Arkansas Bridge Site Background	7
3. Site Response Methodology	9
3.1 Dynamic Site Characterization.....	9
3.2 Input Ground Motions.....	12
3.3 Simulating Wave Propagation.....	14
4. Original Bridge Design Specifications	16
5. 1-D Site Response Analysis Results.....	18
6. Bridge Redesign Based on SSGMRA	22
6.1 61 cm Intermediate Bent Piles	22
6.2 46 cm Intermediate Bent Piles	24
6.3 Other Aspects of Bridge Design.....	26
7. Cost-Savings Analysis.....	27
8. Conclusion.....	30
References.....	32

List of Tables

TABLE 1 - Summary of selected input ground motions [McGuire et al. 2001].	13
TABLE 2 - Load/load effect reduction due to SSGMRA for 61 cm intermediate bent pile design. 23	
TABLE 3 - Load/load effect reduction due to SSGMRA for 46 cm intermediate bent pile design. 25	
TABLE 4 - Cost savings associated with 61 cm intermediate bent piles bridge redesign.	28
TABLE 5 - Cost savings associated with 46 cm intermediate bent pile bridge redesign.	28

List of Figures

FIGURE 1 - Top: Three centuries of earthquakes in Northeast Arkansas [Arkansas Geological Survey 2017] Bottom: Idealized cross section of the Mississippi Embayment [Hashash and Park 2001].	2
FIGURE 2 - Arkansas State owned bridges within respective AASHTO Seismic Performance Zones assuming site classification D. The Monette bridge used for the study is highlighted.	5
FIGURE 3 - Elevation view of Monette Bypass Bridge with restrainer block detail, bent numbering, and soil conditions from ARDOT boring information. N values represent raw blow counts from SPT measurements. Depths are defined as below ground surface (BGS).	8
FIGURE 4 - Top Left – Rayleigh and Love wave experimental dispersion data fit with theoretical curves. Bottom Left – Experimental horizontal to vertical spectral ratio fit with theoretical curves. Right – 1000 lowest misfit shear wave velocity profiles from inversion and 10 randomly selected shear wave velocity profiles used in SSGMRA.	12
FIGURE 5 - AASHTO site class D design spectrum and 2/3 of AASHTO site class D design spectrum with a.) scaled input motions and lognormal median of scaled input motions, b.) equivalent linear analyses results with lognormal median of EQL results, c.) nonlinear analyses results with lognormal median of NL results and d.) LNM of EQL results, LNM of NL results, averaged results, and delineated design spectrum.	19
FIGURE 6 - Maximum shear strains profiles for a.) equivalent linear analyses and b.) nonlinear analyses.	21

1. Introduction

Northeast Arkansas (NEA) is located in the heart of the New Madrid Seismic Zone (NMSZ), an area of the U.S. that has some of the highest design ground motions in the nation. This large seismic hazard is the result of past large magnitude earthquakes occurring within the NMSZ, noted in Figure 1. In addition to the high seismic threat in NEA, the region is located within the upper Mississippi Embayment. This geologic area, also illustrated in Figure 1, is characterized by deep, unconsolidated sedimentary deposits, which form a plunging syncline with an axis that closely traces the course of the Mississippi River [Mento et al. 1986]. The thickness of these deposits ranges from approximately 477 m at New Madrid, Missouri to 987 m at Memphis, Tennessee [Van Arsdale and TenBrink 2000, Rosenblad et al. 2010].

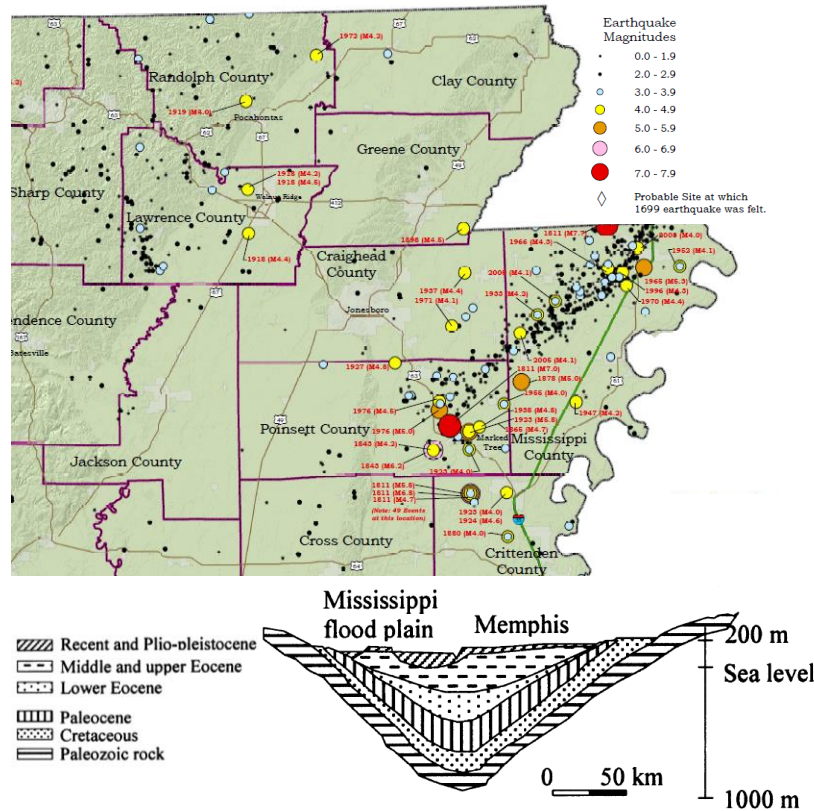


FIGURE 1 - Top: Three centuries of earthquakes in Northeast Arkansas [Arkansas Geological Survey 2017] Bottom: Idealized cross section of the Mississippi Embayment [Hashash and Park 2001].

These two regional characteristics significantly increase the seismic design costs of bridge abutments, deep foundations, and earthquake resisting systems (ERS) in NEA. Currently, the Arkansas Department of Transportation (ARDOT) typically uses the general procedure outlined in the American Association of State Highway and Transportation Officials (AASHTO) Load and Resistance Factor Design (LRFD) Bridge Design Specifications to estimate the seismic demand for highway bridges. Although this methodology usually provides a conservative design, the AASHTO LRFD specifications clearly warn that short-period structures may be over-designed at a significant cost, and long-period structures may be under-designed at a significant risk. This is because the immense sediment thicknesses of the Mississippi embayment are

expected to amplify long-period waves and attenuate short-period waves to a much greater extent than estimated using the general procedure, which only considers the top 30 m of soil [Malekmohammadi and Pezeshk 2015]. Therefore, to better estimate the design ground motions at bridge sites and ensure safe and cost efficient designs, AASHTO recommends conducting a site-specific ground motion response analysis (SSGMRA) for areas such as the Mississippi Embayment. AASHTO specifications directly mention that sites with deep, soft deposits, like those in the Mississippi Embayment, are locations where SSGMRA should be performed. Recognizing the value these types of site specific analyses can add when complex conditions exist, AASHTO allows seismic design forces obtained from general, code based procedures to be reduced by up to 33% if the SSGMRA indicates this is appropriate. Cox et al. [2012] concluded that this reduction could be achieved for short period ranges at bridge sites in NEA, which is where the natural period of most NEA bridges designed by ARDOT fall.

Other research has been conducted to understand the implications of conducting site response at NMSZ bridge sites. Rogers et al. [2007] performed site response analyses at three Missouri River highway bridge sites using artificial acceleration time histories, which predicted site amplification between six and nine times for a large magnitude earthquake. They also concluded that serious foundation failure could occur for earthquakes over M_w 6.5 to 6.6 [Rogers et al. 2007]. However, the bedrock depths for these bridge sites are between 30 m and 40 m, which is much shallower than bedrock depths at bridge sites within the Mississippi Embayment. The deep Mississippi Embayment sedimentary deposits have a very large impact on the transfer of bedrock motions to surface ground motions during a large earthquake [Romero and Rix 2001, Hashash et al. 2010]. The thick sedimentary deposits in NEA are expected to damp out high frequency seismic waves, posing little threat for amplification of short period waves like that seen in the

Missouri River Flood Plain [Cox et al. 2012]. Liu and Stephenson [2004] conducted site response for two bridge sites in the Missouri Bootheel where subsurface soils are more than 600 m thick. They demonstrated the importance of using both equivalent linear (EQL) and nonlinear (NL) site response analyses and the effects of deep soil deposits that cause period migration from short to long periods. This resulted in a broad short period range where site response predicted accelerations less than typical design accelerations. Other Mississippi Embayment site response research also predicts attenuation of short period motions for sites in western Tennessee and Kentucky due to deep unconsolidated sediments [Wang et al. 1996, Harris et al. 1994].

Ketchum et al. [2004] demonstrated the potential cost savings of conducting SSGMRA for post-tensioned box-girder and I-girder bridges, which the California Department of Transportation (CalTrans) typically prefers. Their results show that for typically low overhead bridges, a 5% cost savings can be obtained for each 10% reduction in PGA above a baseline of 0.3 g to 0.4 g. Since AASHTO [2014] allows up to a 33% reduction in the simplified code based design response spectra (including the PGA), based on these results, conducting a SSGMRA could result in a cost reduction on the order of 15% of the total cost of the bridge. This cost savings would be significant for Arkansas bridges within the Mississippi Embayment. Figure 2 illustrates Arkansas state owned bridges within AASHTO seismic performance zones when AASHTO site class D is assumed. Cost savings associated with conducting SSGMRA would be even more significant when the AASHTO seismic performance zone could be lowered from 4 or 3 to 2 or 1 where design requirements are less stringent.

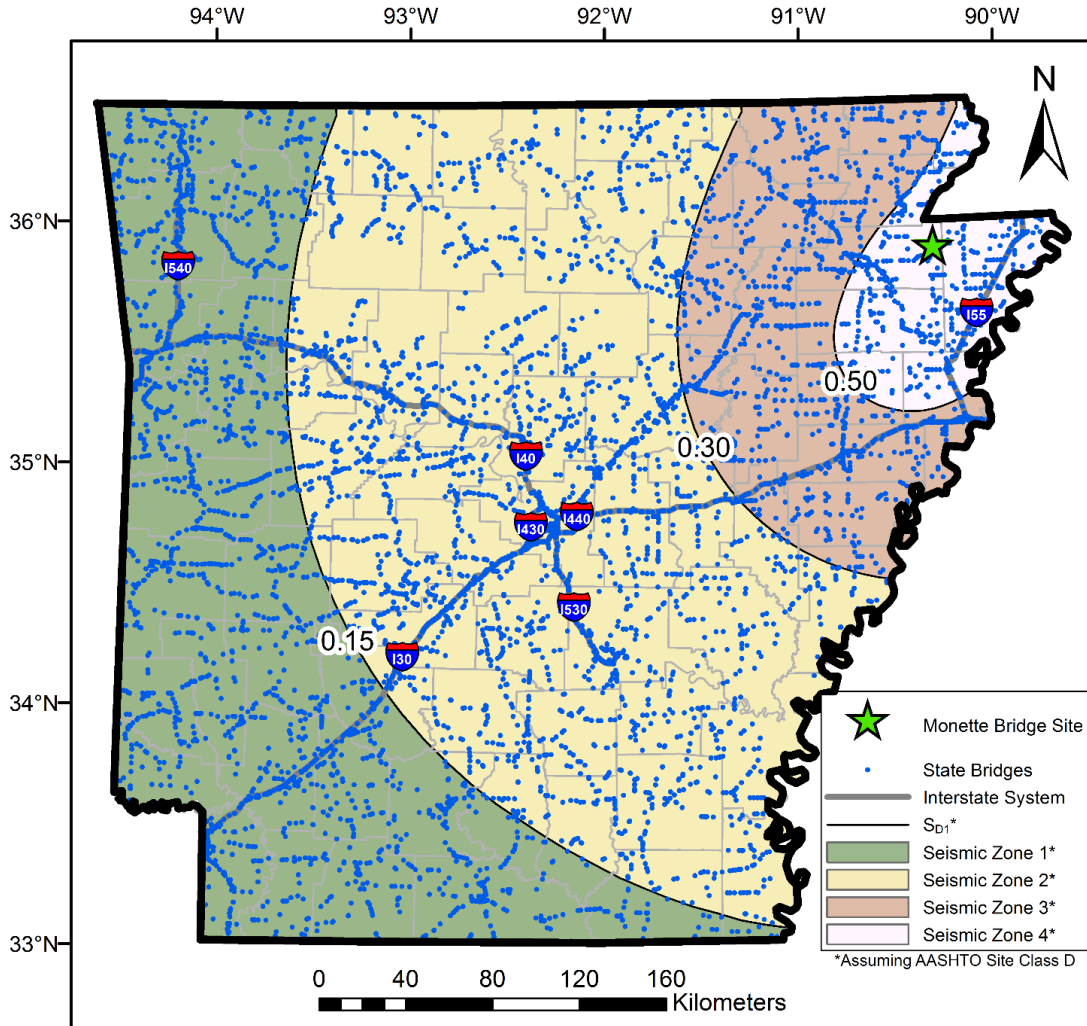


FIGURE 2 - Arkansas State owned bridges within respective AASHTO Seismic Performance Zones assuming site classification D. The Monette bridge used for the study is highlighted.

For this study, deep dynamic site characterization and a SSGMRA were conducted at a recently designed and constructed ARDOT bridge in Monette, Arkansas, which was originally designed using the AASHTO LRFD general procedure. The bridge was then redesigned with the resulting design acceleration response spectrum and the cost-savings associated with conducting the SSGMRA at the Monette bridge was estimated. We first discuss the Monette, Arkansas bridge site background including seismic information and soil conditions along with the site response analysis methodology, including details on obtaining the site-specific shear wave

velocity (V_s) profile and input earthquake acceleration time histories. Then the general aspects of the Monette bridge superstructure and substructure are described, and the highlights of the site response analysis, and details on the bridge redesign based on the SSGMRA results are described. Finally, the cost-savings potential associated with conducting SSGMRA in NEA are presented and discussed.

2. Monette, Arkansas Bridge Site Background

Monette, Arkansas is located on the western edge of Craighead County in NEA as shown in Figure 2. Just east of Monette, Highway 18 crosses the Cockle Burr Slough, a 60 m wide canal that connects into the St. Francis River. Recently, as part of a project that expanded Highway 18 to four lanes and rerouted it to bypass north of Monette, a new 100 m long by 24 m wide bridge was constructed to cross the Cockle Burr Slough. The main components of the bridge include nine 100 m long continuous steel girders and six pile bents. The new structure occupies the same location as the old bridge and was built in stages so that traffic could still flow over the old structure until two lanes of the new bridge could be opened. The lowest bridge chord is 2.5 m above the design flood elevation, which is 2 m higher than the previous structure that crossed the canal. The overall cost of the project was \$13.7 million, of which \$2.82 million was for bridge construction.

The subsurface conditions at the site are characterized by mainly sandy soils with the exception of a clay layer between 3 m and 6 m below existing grade according to ARDOT borings located at each end of the bridge. Some trace gravel exists in layers below 15 m. Soil information at the bridge end bents are detailed in Figure 3. The soil at the site classifies as an AASHTO site class D based on blow count. General procedure design values include a design PGA value of 0.917 g, an S_{DS} value of 1.641 g, and an S_{D1} value of 0.694 g, which corresponds to an AASHTO seismic performance zone of 4. This high seismic hazard is the result of the site's close proximity to the Reelfoot Rift, the main fault system of the NMSZ.

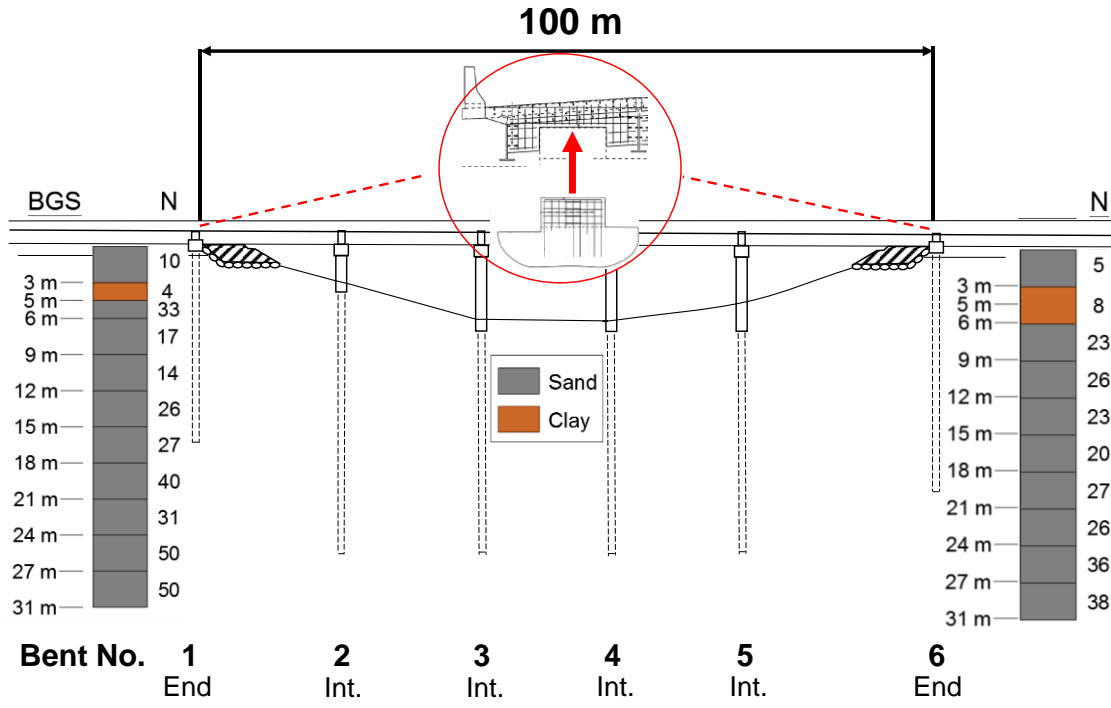


FIGURE 3 - Elevation view of Monette Bypass Bridge with restrainer block detail, bent numbering, and soil conditions from ARDOT boring information. N values represent raw blow counts from SPT measurements. Depths are defined as below ground surface (BGS).

3. Site Response Methodology

To conduct a SSGMRA, there are three main steps: (1) characterize the small-strain V_s of the soil profile down to bedrock, (2) collect and adjust appropriate input earthquake acceleration time histories, and (3) simulate the propagation of input ground motions from bedrock to the ground surface using appropriate numerical analyses. Each of these steps has its own challenges that can contribute to the overall uncertainty in surface ground motion estimates. The following sections discuss each one of these issues for the Monette site.

3.1 Dynamic Site Characterization

To determine the small strain V_s profile at the Monette, Arkansas site, a combination of active source multi-channel analysis of surface waves (MASW), passive source microtremor array measurements (MAM), and horizontal to vertical spectral ratio (HVSr) measurements were carried out. The MASW method was used to collect both Rayleigh and Love surface wave data at the site [Park et al. 1999] with an array of 24, 4.5 Hz vertical (Rayleigh) and horizontal (Love) geophones with a uniform space of 2 m between each geophone (array length of 46 m). Rayleigh and Love waves were generated using vertical and horizontal blows from a 4.5 kg sledgehammer, respectively. To produce high quality data, allow for uncertainty quantification, and to minimize near-field effects, multiple source offsets of 5 m, 10 m, 20 m, and 40 m from the first geophone in the array were utilized. A total of 10 sledgehammer blows were stacked at each source location to improve the signal-to-noise ratio of the recorded waveforms.

MAM measurements were made using circular arrays of ten, three-component Trillium Compact, 20 s broadband seismometers. These seismometers were generally arranged with one seismometer at the center and nine uniformly distributed around the circumference. The exact

location of each seismometer used for testing was recorded using a centimeter accurate GPS unit. Array diameters of 50 m, 200 m, and 500 m were used. Ambient noise was recorded for one hour for the 50 m and 200 m diameter arrays and for two hours for the 500 m diameter array.

Active-source MASW for Rayleigh and Love wave data were processed using the Frequency Domain Beamformer (FDBF) method in combination with the multiple-source offset technique [Zywicki 1999, Cox and Wood 2011]. The use of multiple source offsets during data collection and processing allows for quantifying dispersion uncertainty and the identification of near field contamination. The MAM Rayleigh and Love wave dispersion curves were computed using the HRFK method [Capon 1969] and the MSPAC method [Bettig et al. 2001] from the circular array data. For the MSPAC method, an average dispersion curve was computed for each array from the estimated auto-correlations. The MAM array data were also used to develop HVSRs for each of the ten seismometers for all arrays. Ambient records were processed in general accordance with SESAME [2004]. Once all dispersion data from each method were developed, data were combined to form a mixed-method composite experimental dispersion curve as shown for Rayleigh and Love waves in Figure 4.

The composite experimental dispersion curve and HVSR peak for each site were used in a joint inversion using the Geopsy software package, Dinver [Wathelet et al. 2008]. Dinver operates by generating trial V_s profiles using a neighborhood algorithm [Thomson 1950, Haskell 1953, Dunkin 1965, Knopoff 1964] within user-defined constraints. The layer parameterization at each site was developed based on the geologic layer boundaries and geologic materials from the Central United States Seismic Velocity model detailed in Ramirez-Guzman et al. [2012]. A range of velocity, density, and Poisson's ratio values for each layer were estimated based on the type of material expected in each geologic strata. V_s values for each layer were defined based on

V_s reference curves from Lin et al. [2014], which are dependent on soil type and mean effective confining pressure. Poisson's ratio was allowed to vary between 0.25-0.35 for soils above the water table. Poisson's ratio for soils below the water table was based on a V_p of 1500 m/s in the near surface, however at depths where V_s was greater than 750 m/s, V_p was allowed to increase beyond 1500 m/s to constrain Poisson's ratio between the range of 0.25-0.35 which is typical for dense sand and gravel layers present at these depths [Coduto 1999]. A uniform density of 2000 kg/m³ was used for soils and 2300 kg/m³ for bedrock.

For the inversion, two million trial V_s profiles were used to generate Rayleigh and Love wave dispersion curves and ellipticity curves in an effort to obtain the closest dispersion curve fit based on a misfit calculation, which is a function of the dispersion and HVSR fit. The theoretical fits for the Rayleigh, Love, and HVSR experimental data are shown in Figure 4 for the 1000 lowest misfit V_s profiles. The 1000 lowest misfit V_s profiles are also shown in Figure 4. To conduct the SSGMRA, 10 V_s profiles (shown in green in Figure 4), were randomly selected from the top 1000 lowest misfit profiles. The variability in these profiles was used to account for uncertainty in a more meaningful way than the industry standard approach of using median and $\pm 20\%$ profiles [Griffiths et al. 2016b]. Using V_s profiles that extend to bedrock has been shown to be critical to properly estimating the ground motions for sites within the Mississippi Embayment [Cramer et al. 2004; Hashash and Park 2001]. For further information regarding the data collection or processing, please see Wood et al. [2014] or Deschenes et al. [2018].

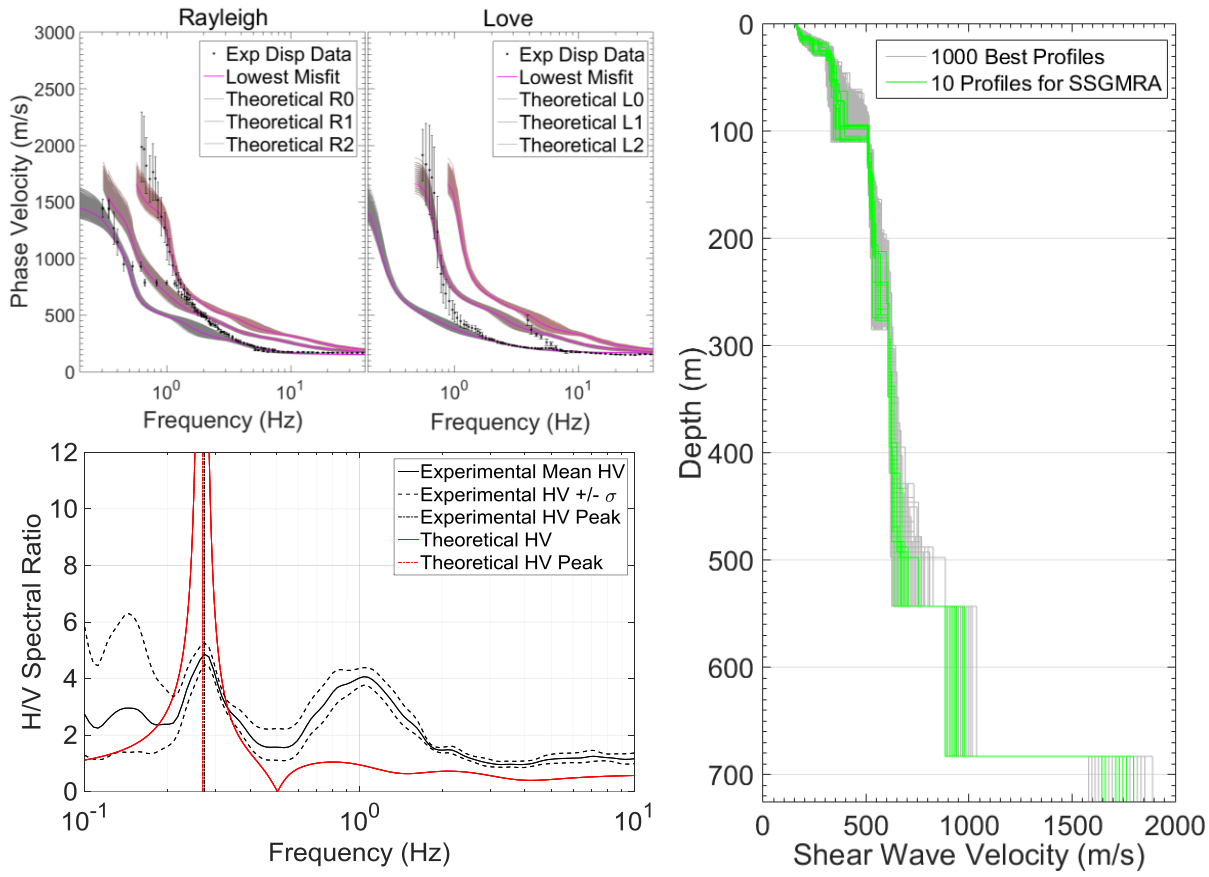


FIGURE 4 - Top Left – Rayleigh and Love wave experimental dispersion data fit with theoretical curves. Bottom Left – Experimental horizontal to vertical spectral ratio fit with theoretical curves. Right – 1000 lowest misfit shear wave velocity profiles from inversion and 10 randomly selected shear wave velocity profiles used in SSGMRA.

3.2 Input Ground Motions

A deaggregation was performed using the USGS Unified Hazard Tool. Deaggregation results indicated that a singular scenario governs the seismic hazard at all periods: a modal magnitude 7.7 earthquake at a distance between 22 km and 23 km. The Unified Hazard Spectrum (UHS) was chosen as the design target spectrum, which is an appropriate target spectrum if conservative estimates of response are acceptable [NEHRP 2011].

The AASHTO Guide Specifications for LRFD Seismic Bridge Design state that response-spectrum-compatible time histories shall be developed from representative recorded earthquake

motions. Rathje et al. [2010] argued that these time histories have the greatest influence on site response results. Large magnitude ground motions at short distances have never been recorded in the Central United States. Therefore, as part of a Nuclear Regulatory Commission project, earthquake acceleration time histories from various regions were adjusted to encompass the frequency content expected from an earthquake occurring in the Central and Eastern United States [McGuire et al. 2001]. The selected input acceleration time histories from McGuire et al. [2001] were restricted to those with magnitudes and distances consistent with the deaggregation [Kramer 2012]. Ultimately, ten input ground motions, listed in Table 1, were selected.

TABLE 1 - Summary of selected input ground motions [McGuire et al. 2001].

File Name	EQ	PGA (g)	Magnitude M_w	Distance R (km)	Duration (s)
SHL090	Cape Mendocino	0.585	7.1	33.8	14.6
SHL000	Cape Mendocino	0.648	7.1	33.8	14.4
GBZ000	Kocaeli, Turkey	0.454	7.4	17	7.3
DAY-TR	Tabas, Iran	0.947	7.4	17	9.7
DAY-LN	Tabas, Iran	0.993	7.4	17	8.8
GYN000	Kocaeli, Turkey	0.313	7.4	35.5	8.3
TCU128-N	Chi-Chi, Taiwan	0.305	7.6	9.7	29.9
TCU046-W	Chi-Chi, Taiwan	0.336	7.6	14.3	18.8
TCU047-W	Chi-Chi, Taiwan	0.7	7.6	33	12.9
TCU047-N	Chi-Chi, Taiwan	1.168	7.6	33	10.8

RspMatch [2009] was used to match the ten selected ground motions to the UHS target spectrum [Hancock et al. 2006]. According to AASHTO [2011], input rock acceleration time histories should be adjusted, either by scaling or spectral matching, to match the seismic hazard

consistent with the bridge site. Advantages to spectral matching include reduction of record-to-record variability, which reduces output variability and also enhancement of select frequencies with no unconservative bias in response [NEHRP 2011].

3.3 Simulating Wave Propagation

To perform the site response analysis, the software program DEEPSOIL 6.1 was utilized. It has been shown to produce appropriate site response results for sites with deep sedimentary deposits, such as those in the Mississippi Embayment, because of its short period accuracy [Zheng et al. 2010, Hashash and Park 2001].

Within DEEPSOIL, a new model for small-strain nonlinearity and strength, termed the GQ/H model, has recently been implemented [Groholski et al. 2016]. The GQ/H model allows users to define target shear strengths for each layer and satisfies both the small-strain and large-strain modeling of the soil backbone curve. It does so by following a fitting procedure that slightly increases the shear modulus reduction curve from the reference curve at higher strains. This eliminates the need for manually implied shear strength corrections, which were previously required in older models to account for strain-hardening behavior. The GQ/H model was used to fit corrected curves to the Darendeli [2001] modulus reduction and damping curves for each soil layer. These dynamic soil properties were not randomized because no reasonable variability parameters could be determined [Malekmohammadi and Pezeshk 2015].

Soil type, plasticity, and blow count information was obtained from ARDOT boring logs and used in calculations for dynamic soil properties. For layers below the final boring depth, sand reference curves for normally consolidated sands were assigned. Target shear strength values were estimated using either a SPT blow count to shear strength correlation based on ARDOT

boring logs or a Mohr-Coulomb behavior shear strength assuming a friction angle of 30° and no cohesion.

Due to the limitations and advantages of each type of analysis, EQL and NL analysis results were weighted equally to obtain an overall design response spectrum. EQL analyses can produce a very flat response at high frequencies due to high damping values at sites where high shear strains are expected [Griffiths et al. 2016a], and underestimates ground motions at high frequencies for thick soil deposits [Romero and Rix 2001]. NL analyses can better predict soil behavior under large strains from strong ground motions at soft soil sites because it accounts for changes in soil properties at each time step [Kim et al. 2016]. However, EQL analysis is still the most common method in practice [Rathje et al. 2010] and has proved to be valuable for studies within the NMSZ [Liu and Stephenson 2004].

4. Original Bridge Design Specifications

The superstructure of the Monette bypass bridge, presented in Figure 3, consists of a 22 cm thick deck slab and nine 100 m long continuous W36x135, Grade 50W steel girders spaced at 2.75 m. The girders are supported by two end stub abutments (termed end bents herein) and four intermediate pile-bents, and are equipped with bumper bars, which are assumed to transfer the lateral load to the substructure by striking against a steel bumper plate attached to the end bents during seismic excitation.

An important aspect of the composite deck is the concrete restrainer block system, also illustrated in Figure 3. The restrainer blocks, the bridge's main earthquake resisting system (ERS), are designed to resist transverse seismic loads. At end abutments, concrete was cast over the first 45 cm of the girders and diaphragms leaving approximately 13 cm of web and bottom flange exposed. Subsequently, four 63.5 cm tall by 137.2 cm wide restrainer blocks were cast on top of the end bents. With this interlocking system of the composite deck and the abutments, transverse movement is restricted during a seismic event.

Nine 46 cm (18 in) diameter closed end concrete filled steel pipe piles of 1.25 cm (0.5 in) wall thickness are integrated into the bottom of each end bent. Similarly, nine 61 cm (24 in) x 1.25 cm inch closed end concrete filled steel pipe piles are integrated into the bottom of each of the four intermediate bents.

From WinSEISAB®, a dynamic analysis program that analyzes bridge structures to determine the seismic demand placed on various bridge components [WINSEISAB 2009], the bridge has a longitudinal period of 1.272 s and a transverse period of 0.365 s before joint lockup. After joint lockup, the longitudinal period changes to 0.360 s. The program also outputs mass

participation per mode and total accumulated mass participation along with the vibration characteristics of the structure.

5. 1-D Site Response Analysis Results

A delineated design response spectrum was developed and shown in Figure 5d for the Monette site using the site response acceleration response spectrum, the upper limiting AASHTO site class D design response spectrum, and the lower limiting two-thirds AASHTO site class D design response spectrum. The scaled input motions are shown in Figure 5a, the EQL results are shown in Figure 5b, the NL results are shown in Figure 5c, and the combined EQL and NL results are shown in Figure 5d. The delineated design response spectrum is the greater of either the site-specific response spectrum or two-thirds of the general response spectrum and is always less than or equal to the AASHTO site class D response spectrum obtained from the general procedure.

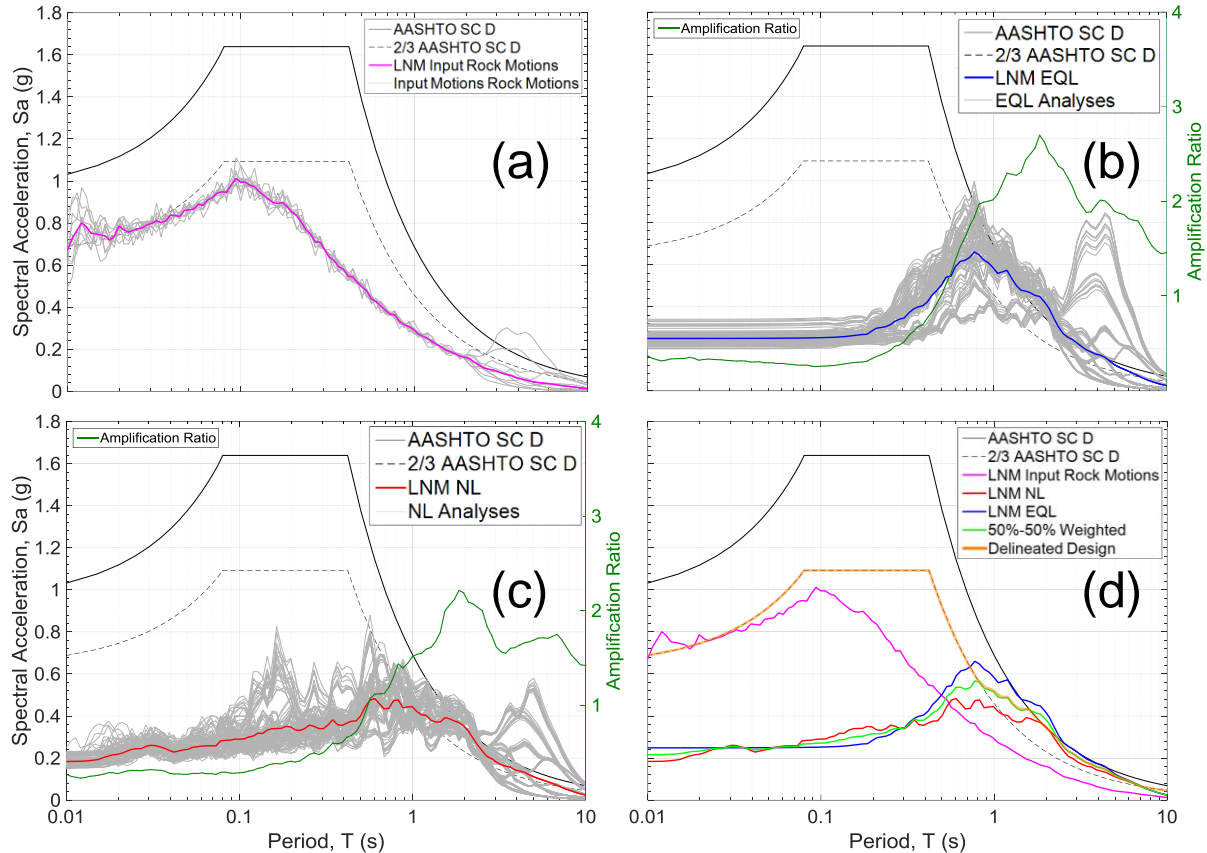


FIGURE 5 - AASHTO site class D design spectrum and 2/3 of AASHTO site class D design spectrum with a.) scaled input motions and lognormal median of scaled input motions, b.) equivalent linear analyses results with lognormal median of EQL results, c.) nonlinear analyses results with lognormal median of NL results and d.) LNM of EQL results, LNM of NL results, averaged results, and delineated design spectrum.

Results from this analysis indicate a generally flat response from the PGA to approximately 0.2 s. The EQL analysis response spectrum begins to exceed the two-thirds AASHTO Site Class D design spectrum at around 0.7 s – 0.8 s, which is similar to the results presented in Cox et al. [2012] for a Blytheville, Arkansas site. The NL response spectrum begins to exceed the two-thirds AASHTO design spectrum around 1.0 s. As expected, the NL analyses resulted in lower accelerations than the EQL analyses for most periods. The smooth peak of the site response spectrum indicates that no wave energy entrapment is expected for the soft soil site.

Also illustrated in Figure 5b and c, amplification of input rock motions begins around 0.5 s and continues until a peak amplification of 2.7 times and 2.2 times is reached at 1.85 s for EQL and NL analyses, respectively. This amplification is consistent with that observed in Cox et al. [2012]. Rogers et al. [2007] also observed this type of period migration for three Missouri River highway bridge sites. This causes higher potential for constructive interference with long period bridges. The deamplification from PGA to 0.5 s is also noteworthy. Design of structures in NEA with a natural period in this range will benefit from the lower design spectral acceleration estimated by a SSGMRA compared to those estimated using the general procedure. This attenuation is also consistent with previous Mississippi Embayment SSGMRA research [Cox et al. 2012, Liu and Stephenson 2004, Zheng et al. 2010, Malekmohammadi and Pezeshk 2015].

Maximum strain levels reached 1.57% for EQL analyses and 1.54% for NL analyses as shown in Figure 6. The TCU128-N record ($M_w = 7.6$ in Chi-Chi, Taiwan) produced the highest maximum shear strains out of all of the selected input records. This record has the longest duration and shortest distance from fault rupture of all the records. It was also among records with the highest magnitudes. Zheng et al. [2010] observed similar shear strain magnitudes using their average V_s profile for Osceola, AR. These shear strain values are less than those observed by Cox et al. [2012], but the input ground motion was greater for their Blytheville site versus the Monette site.

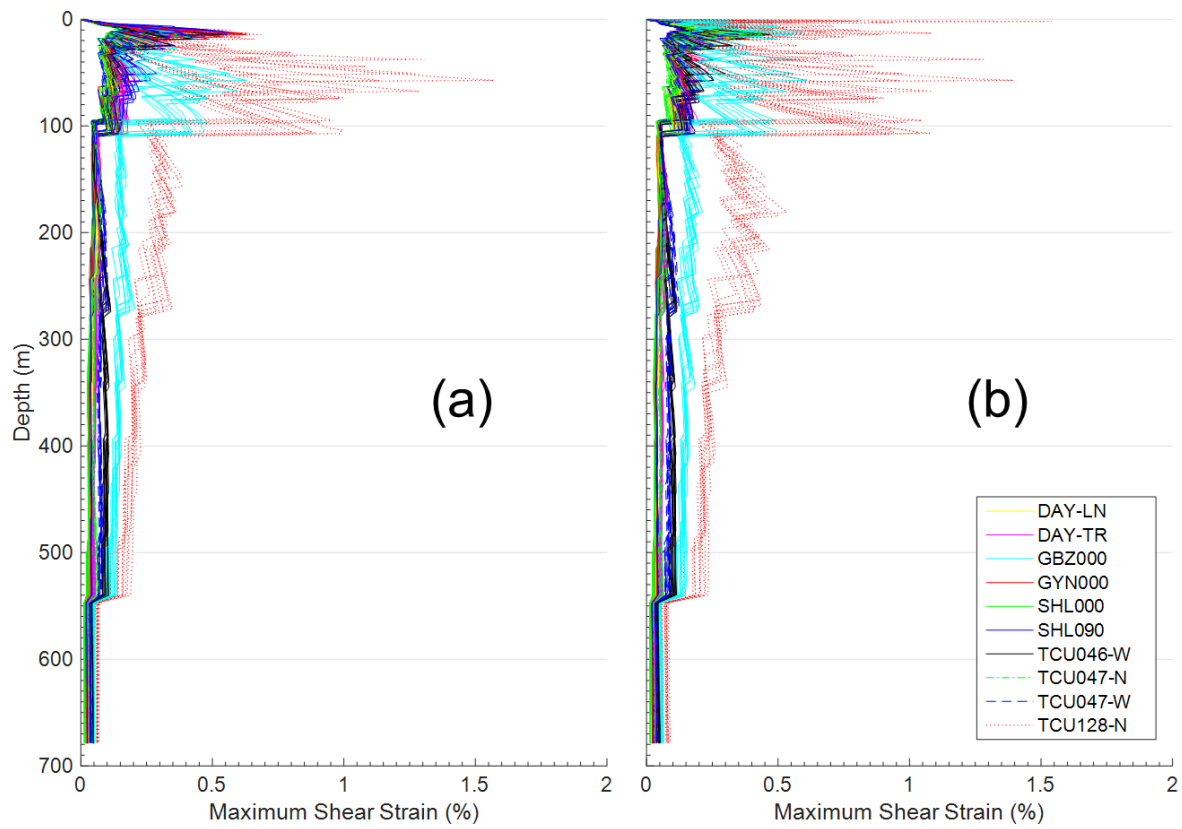


FIGURE 6 - Maximum shear strains profiles for a.) equivalent linear analyses and b.) nonlinear analyses.

6. Bridge Redesign Based on SSGMRA

Four major components of the bridge project were considered in the seismic redesign: restrainer blocks, columns, piles, and approach embankment. While there may be additional components that would benefit from being redesigned using the post SSGMRA response spectrum, these likely would result in limited cost savings compared to the components mentioned above. The redesign of each of the components used the same ARDOT design methodology as the original project to yield the most accurate cost savings values for the redesign. To maintain the intricacies of the original structure, which is important for the cost-savings analysis, two redesign options were considered that used similar components as the original design. These two options were (1) use 61 cm diameter intermediate bent piles and 46 cm end bent piles (same design as original structure), or (2) downsize the intermediate bent piles to 46 cm diameter piles, which uses only 46 cm piles for the entire structure. These two options are discussed below in detail.

6.1 61 cm Intermediate Bent Piles

A new dynamic analysis was performed in WinSEISAB® [WINSEISAB 2009] using the delineated design acceleration response spectrum from the SSGMRA. The reduction in notable loads and load effects is outlined in Table 2. From this analysis, there is a linear type of relationship between the reduction in design accelerations and some seismic forces/effects. In particular, column axial load, column transverse moment, and lateral force on restrainer blocks were all reduced by approximately 33% (i.e., the same reduction in the short period range of the updated design response spectrum).

TABLE 2 - Load/load effect reduction due to SSGMRA for 61 cm intermediate bent pile design.

	Load/Effect	Pre SSGMRA	Post SSGMRA	Unit	% Reduction	Location/ Load Case	AASHTO Methods/ Criteria
Restrainer Block Design	$F_{T \text{ Max}}$	13340	8892	kN	33.3%	Load Case 4	5.7.5 5.8.3.3 5.8.4
Column Design	P_{max}	1468	979	kN	33.3%	Bent 3, Column 4, LC 4	6.9.5.1 4.5.3.2.2b 6.12.2.2.3 6.9.2.2 4.7.4.5
	$M_{T \text{ Max}}$	629	419	$kN-m$	33.3%	Bent 3, Column 4, LC 4	
	$M_{L \text{ Max}}$	168	149	$kN-m$	11.3%	Bent 2 Column 1, LC3	
Pile Length Design	P_{required}	2358	1922	kN	18.5%	Interior Bent Piles (2-5)	
	P_{required}	605	458	kN	24.3%	End Bent Piles (1,6)	

The reduction in lateral forces on the bridge allowed a reduction in restrainer block size. The height and transverse width of the blocks were reduced while the lateral width of the blocks were not adjusted. From a construction perspective, it is easier to cast the blocks flush with the face of the abutment. The height of the blocks was reduced from 63.5 cm to 53 cm, and the transverse width was reduced from 137 cm to 89 cm. Shear and moment reinforcement was redesigned considering the reduction in lateral forces, which resulted in a reduction of about 450 kg of rebar.

For the columns, 0.16 cm section loss was assumed due to corrosion or scour. Since the columns were structurally sound as 61 cm diameter piles with the original seismic load, they were satisfactory for the reduced seismic load. The axial pile capacity was then checked while considering the effect of potentially liquefiable layers. With the reduction in PGA, liquefaction hazard was reanalyzed. ARDOT utilizes a deterministic approach for liquefaction analysis.

Liquefaction potential was evaluated using SPT blow counts for the Youd et al. [2001], Cetin et

al. [2004], and Idriss and Boulanger [2008] methods. However, little difference in potentially liquefiable layers was observed between the methods due to the poor soils at the site. One layer between 6 m and 7.6 m at bent 6 changed from potentially liquefiable ($FS < 1$) to non-liquefiable ($FS > 1$) when considering the reduced SSGMRA PGA.

DRIVEN® [DRIVEN 2001] was used to input the soil profile from boring log information and to determine the pile capacities at given depths. The skin friction resistance of the pile was reduced in layers at which the factors of safety for liquefaction were less than 1.0. Even though there was only small change in the potentially liquefiable layers, the reduction in axial load caused some piles to reach required capacity at shallower depths than in the original design. The intermediate bent pile lengths were reduced by 1.2 m each, resulting in a total reduction of 44 m of 61 cm diameter piling. The greatest length change was estimated at bent 6. The original bent 6 piles reached the required axial capacity at 15.25 m. However, since piles are not allowed to bear in liquefiable layers, the design length of these piles had to be extended through the liquefiable layer to 20 m. The reduced axial load from SSGMRA allowed the piles to reach the required capacities at 12.8 m and bear in a dense sand layer. This resulted in a total reduction of 63 m of 46 cm diameter pipe piling. The complex soil layering at bent 1 prevented any reduction in pile length. It should be noted that the pile length reductions are based on design calculations and true as-built pile lengths may vary. However, the as-built length is likely to be reduced by a similar amount compared to the design lengths due to the decreased axial demand.

6.2 46 cm Intermediate Bent Piles

The dynamic analysis for the structure with 46 cm diameter intermediate bent piles showed an even larger reduction in column loads than the 61 cm diameter intermediate bent pile

structure. However, restrainer block forces and pile forces were not reduced as significantly. The pre and post SSGMRA loads for the 46 cm diameter intermediate bent pile structure are presented in Table 3.

TABLE 3 - Load/load effect reduction due to SSGMRA for 46 cm intermediate bent pile design.

Design	Load/Effect	Pre SSGMRA	Post SSGMRA	Unit	% Reduction	Location	AASHTO Methods/ Criteria
Restrainer Block Design	$F_{T \text{ Max}}$	13337	11555	kN	13.4%	Load Case 4	5.7.5 5.8.3.3 5.8.4
Column Design	P_{max}	1469	725	kN	50.7%	-	6.9.5.1 4.5.3.2.2b 6.12.2.2.3 6.9.2.2 4.7.4.5
	$M_{T \text{ Max}}$	629	217	$kN-m$	65.5%	-	
	$M_{L \text{ Max}}$	168	55	$kN-m$	67.4%	-	
Pile Length Design	P_{required}	2356	1595	kN	32.3%	Interior Bent Piles (2-5)	6.9.2.2 4.7.4.5
	P_{required}	604	580	kN	4.0%	End Bent Piles (1,6)	

Even though the reduction in lateral forces was not as great as for the 61 cm diameter column structure, a reduction in restrainer block size was still achieved. The height of the blocks was reduced from 63.5 cm to 58.5 cm, and the transverse width was reduced from 137 cm to 89 cm. There was also a reduction in the reinforcement needed, which amounted to about a 220 kg reduction in rebar.

The axial loads and moments were found for several different columns on respective bents and load cases in order to capture the design load envelope. The magnified moments and flexural resistance of the pile was calculated. Then, the combined axial compression and flexural resistance was checked for the several different columns and load cases. Displacement

requirements (P- Δ) were then checked. Other significant limit states, such as Strength I, were also satisfied.

With the large reduction in load/load effects for the columns comes a reduction in section capacity. However, the 46 cm diameter piles were determined to be satisfactory as columns. The designs for the end bents (bents 1 and 6) are the same as those for the 61 cm diameter column redesigned structure. This is due to both end bent piles being 46 cm in diameter for both cases, and the change in seismic load between the two structures is relatively small because of their fully supported lengths. Intermediate pile lengths were reduced by 1.2 m each compared to the original pile lengths. Lengths were again reduced for bent 6 piles by about 7 m compared to the original ARDOT design. Again, pile lengths at bent 1 could not be reduced.

6.3 Other Aspects of Bridge Design

It is important to note other bridge aspects that could benefit from reduced seismic demand. In particular, the seismic design of the bridge approach embankments that are design based on a seismic slope stability analysis. Reducing this design PGA, would provided a potential cost savings. For the original design, slope stability analyses were conducted for the embankments which indicated 8 layers of 130 kN/m geogrid reinforcement on 30.5 cm vertical spacing and extending 30 meters beyond the abutment were required to satisfy stability requirements. Using the updated SSGMRA PGA, stability of the embankment was achieved using 4 layers of 30 kN/m geogrid reinforcement on 30.5 cm vertical spacing and extending 30 meters beyond the abutment. This significantly reduced both the quality (lower tensile strength) and quantity (approximately half the area required) of geogrid required for the job.

7. Cost-Savings Analysis

Cost savings analyses was conducted using both redesign options discussed above. Tables 4 and 5 outline the cost savings for each analysis compared to the original bid items for the 61 cm structure and 46 cm structure, respectively. The redesign savings, which is directly based on the original bid documents for the structure with 61 cm diameter intermediate piles are outlined in Table 4. A total savings of \$164,089 was determined for this bridge redesign, which represents a 5.82% reduction in the cost of the project with respect to the original bid. The savings for the structure with 46 cm diameter intermediate piles are listed in Table 5. A total savings of \$206,992 was determined for this structure, which represents a 7.34% reduction in the cost of the project. These cost reductions are consistent with other findings from Ketchum et al. (2004). The majority of the savings for each structure is from the reduction in pile lengths and sizes as well as the reduction in strength and area of embankment reinforcement. A slight savings from the reduction in restrainer block design was also estimated.

TABLE 4 - Cost savings associated with 61 cm intermediate bent piles bridge redesign.

Original Design					61 cm Intermediate Bent Piles			
Quantity	Unit	Item	Winning Bid Unit Cost	Total	Redesign Quantity	Unit Cost	Total	Savings
206	CU M	CLASS S CONCRETE-BRIDGE	\$921.57	\$189,927	204	921.57	\$ 187,622.36	\$2,304.65
14510	KG	REINF STEEL BRIDGE (GR 60)	\$2.64	\$38,352	14283	2.64	\$37,752	\$600
76563	KG	EPOXY COATED REINF STEEL (GRADE 60)	\$2.42	\$185,504	76336	2.42	\$184,954	\$550
329	M	STEEL SHELL PILING (18" DIAM)	\$409.84	\$135,000	266	409.84	\$109,125	\$25,875
933	M	STEEL SHELL PILING (24" DIAM)	\$459.02	\$428,400	889	459.02	\$408,240	\$20,160
18894	SQ M	EMBANKMENT REINFORCEMENT	\$7.18	\$135,600.00	8778	2.39	21000	\$114,600
				TOTAL BRIDGE COST	\$ 2,821,743.30	TOTAL SAVINGS		\$ 164,089.65
						% SAVINGS		5.82%

TABLE 5 - Cost savings associated with 46 cm intermediate bent pile bridge redesign.

Original Design					46 cm Intermediate Bent Piles			
Quantity	Unit	Item	Winning Bid Unit Cost	Total	Redesign Quantity	Unit Cost	Total	Savings
206	CU M	CLASS S CONCRETE-BRIDGE	\$921.57	\$189,927	204	921.57	\$187,884.62	\$2,042.39
14510	KG	REINF STEEL BRIDGE (GR 60)	\$2.64	\$38,352	14396	2.64	\$38,052	\$300
76563	KG	EPOXY COATED REINF STEEL (GRADE 60)	\$2.42	\$185,504	76449	2.42	\$185,229	\$275
329	M	STEEL SHELL PILING (18" DIAM)	\$409.84	\$135,000	1156	409.84	\$473,625	-\$338,625
933	M	STEEL SHELL PILING (24" DIAM)	\$459.02	\$428,400	0	459.02	\$0	\$428,400
18894	SQ M	EMBANKMENT REINFORCEMENT	\$7.18	\$135,600.00	8778	2.39	21000	\$114,600
				TOTAL BRIDGE COST	\$ 2,821,743.30	TOTAL SAVINGS		\$ 206,992.39
						% SAVINGS		7.34%

For both the 61 cm diameter column structure and the 46 cm diameter column structure, no cost savings was attributed to liquefaction analysis. Only one layer, which is at bent 6 from 6 to 7.5 m, changed from liquefiable to non-liquefiable when considering the reduced PGA from

SSGMRA. This layer contributes very little skin friction capacity even when considered as non-liquefiable. Therefore, the reduction in cost by reducing the pile length was primarily a result of the reduced axial load from SSGMRA.

Embankment design savings were calculated by comparing the pre-SSGMRA Geogrid requirements with the post-SSGMRA requirements. Based on information provided by Tensar, a unit cost of \$7.18/SM was used for the 130 kN/m Geogrid and a unit cost of \$2.39/SM was used for the 30 kN/m Geogrid. Ultimately, this resulted in a \$114,600 savings for the embankment design.

From the findings of this research, a gross cost savings of approximately \$205,000 was estimated for the Monette, AR bridge as a result of performing SSGMRA. This estimate is expected to vary by project as the original design details, such as the relationship of S_{D1} to performance zone boundaries, location of liquefiable layers, original factor of safety of liquefiable layers, embankment requirements, site classification, and site specific soil conditions, all play a role in the potential cost savings associated with conducting a SSGMRA. The net cost savings for performing a future SSGMRA for bridge construction should consider the additional cost of performing the SSGMRA.

8. Conclusion

In this study, deep dynamic site characterization using surface wave and HVSR techniques was conducted at an ARDOT bridge site in Monette, AR, which is located within the Mississippi Embayment. The V_s profiles developed to bedrock (depth of 680 meters) were used to conduct a SSGMRA for the bridge site using a combination of equivalent linear and completely nonlinear site response analyses in DeepSoil in accordance with AASHTO 3.10.2.2. The results from both analyses demonstrate the attenuation of high frequency seismic waves and the amplification of long period waves within the deep sediments of the Mississippi Embayment. This attenuation at short periods lead to a reduction in the design acceleration response spectrum for the bridge of 1/3 (AASHTO lower bound limit of 2/3 of the general procedure design response spectrum) in the short period range ($\sim < 1.0$ seconds) for the Monette, AR site. Using the updated design response spectrum from SSGMRA, several aspects of the bridge were redesigned including the restraining blocks, bents/columns, piles and pile lengths, and approach embankments. For each aspect, the size and/or quantity of the design element was able to be reduced. Using the original unit bid prices, a cost-savings analysis was conducted. The majority of the cost savings associated with conducting the SSGMRA was related to reducing the length/size of piling for the bridge ($\sim \$90,000$ savings) and a reduction in the quantity and quality of geogrid required to reinforce the approach embankment ($\sim 114,000$ savings). This resulted in a total gross potential cost-savings for the Monette bridge of $\$205,000$, or approximately 7% of the original bid price of the project.

While this demonstrates the significant potential cost savings associated with conducting a SSGMRA for bridges located in the Mississippi Embayment, there are a number of complex factors that play a role in whether a SSGMRA will provide a cost-savings benefit to a project.

Assuming that a significant cost-savings will be achieved for all Mississippi Embayment bridges is not appropriate. Complex variables including the magnitude of the PGA, the S_{D1} value used in determining seismic performance zone, soil liquefaction potential, bridge length and structural type, foundation type, depth to bedrock, and other items all play a role in determining the benefit of conducting a SSMGRA. Additional research is needed to determine the detailed influence of these parameters on the potential cost savings of conducting a SSGMRA.

References

- American Association of State Highway and Transportation Officials (AASHTO). [2014] “AASHTO LRFD Bridge Design Specifications,” 7th ed., Washington, D.C.
- American Association of State Highway and Transportation Officials (AASHTO). [2011] “Guide Specifications for LRFD Seismic Bridge Design,” 2nd ed. Washington, D.C.
- Arkansas Geological Survey. [2017] “Three Centuries of Earthquakes in Arkansas from 1699 through 2016,”
http://www.geology.ar.gov/maps_pdf/geohazards/Arkansas_Seismicity_Map.pdf
- Bettig, B., Bard, P.Y., Scherbaum, F., Riepl, J., Cotton, F., Cornou, C., and Hatzfield, D. [2001] “Analysis of dense array noise measurements using the modified spatial auto correlation method (SPAC): application to the Grenoble area.” *Bollettino de Geofisica Teoria e Applicata*, 42(3-4), 281-304.
- Capon, J. [1969] “High Resolution Frequency-Wavenumber Spectrum Analysis,” *Proceedings of IEEE*, 57(8), 1408–1418.
- Cetin, K.O., Seed, R.B., Kiureghain, A.D., Tokimatsu, K., Harder, L.F., Kayen, R.E., and Moss, R.E.S. [2004] “Standard Penetration Test-Based Probabilistic and Deterministic Assessment of Seismic Soil Liquefaction Potential,” *Journal of Geotechnical and Geoenvironmental Engineering* 130(12), 1314-1340.
- Coduto, D. P. [1999] *Geotechnical Engineering: Principles and Practices*, Prentice-Hall, Inc. Upper Saddle River, New Jersey 07458, 320.
- Cox, B.R., Ellis, T.B., and Griffiths, S.C. [2012] “Site-Specific Seismic Ground Motion Analyses for Transportation Infrastructure in the New Madrid Seismic Zone,” Mack-Blackwell Rural Transportation Center.
<http://ww2.mackblackwell.org/web/research/ALL_RESEARCH_PROJECTS/3000s/3032/MBTC-3032FinalReport.pdf>
- Cox, B., Wood, C. [2011] “Surface wave benchmarking exercise: methodologies, results, and uncertainties.” *GeoRisk 2011: Geotechnical Risk Assessment and Management*. 845-852

Cramer, C.H., Gomberg, J.S., Schweig, E.S., Waldron, B.A., and Tucker, K. [2004] “The Memphis, Shelby County, Tennessee, Seismic Hazard Maps,” U.S. Geological Survey Open File Report 2004-1294.

Darendeli, M. [2001] “Development of a New Family of Normalized Modulus Reduction and Material Damping Curves,” Ph.D. Dissertation, Civil Engineering Dept., University of Texas, Austin, Texas.

Deschenes, M., Wood, C., Wotherspoon, L., Bradley, B., Thomson, E. [2018] “Development of deep shear wave velocity profiles in the Canterbury Plains, New Zealand,” Earthquake Spectra (in review).

DRIVEN (1.2) [2001]. Computer software. Logan, UT: Blue-Six Software, Inc. Federal Highway Administration.

Dunkin, J.W. [1965] “Computation of modal solutions in layered, elastic media at high frequencies,” Bulletin of the Seismological Society of America, 55, 335–358.

Griffiths, S.C., Cox, B.R., Rathje, E.M. [2016] “Challenges associated with site response analyses for soft soils subjected to high-intensity input ground motions,” Soil Dynamics and Earthquake Engineering 85, 1-10.

Griffiths, S.C., Cox, B.R., Rathje, E.M., Teague, D.P. [2016] “Mapping Dispersion Misfit and Uncertainty in V_s Profiles to Variability in Site Response Estimates,” Journal of Geotechnical and Geoenvironmental Engineering 142(11), 04016062 1-12.

Groholski, D.R., Hashash, Y.M.A, Kim, B., Musgrove, M., Harmon, J., Stewart, J. [2016]. “Simplified Model for Small-Strain Nonlinearity and Strength in 1D Seismic Site Response Analysis,” Journal of Geotechnical and Geoenvironmental Engineering 142(9), 04016042 1-14.

Hancock, J., Watson-Lamprey, J., Abrahamson, N., Bommer, J.J., Markatis, A., McCoy, E., Mendis, R. [2006] “An Improved Method of Matching Response Spectra of Recorded Earthquake Ground Motion Using Wavelets,” Journal of Earthquake Engineering 10(1), 67-89.

Harris, J.B., Street, R.L., Kiefer, J.D., Allen, D.L., Wang, Z.M. [1994] “Modeling Site Response in the Paducah, Kentucky Area,” Earthquake Spectra 10(3), 519-538.

- Hashash, M.A., Park, D. [2001] "Non-linear one-dimensional seismic ground motion propagation in the Mississippi Embayment," *Engineering Geology* 62, 185-206.
- Hashash, Y., Phillips, C. and Groholski, D. [2010] "Recent Advances in Non-Linear Site Response Analysis," *Proc. of the Fifth International Conference on Recent Advances in Geotechnical Earthquake Engineering and Soil Dynamics, San Diego, California, OSP 4 22 pp.*
- Haskell, N. A. [1953] "The dispersion of surface waves on multilayered media, *Bulletin of Seismological Society of America*," 43, 17–34.
- Idriss, I. M., and Boulanger, R. W. [2008] "Soil Liquefaction during Earthquakes," *Earthquake Engineering Research Institute, MNO- 12.*
- Kim, B., Hashash, Y.M.A., Stewart, J.P., Rathje, E.M., Harmon, J.A., Musgrove, M.I., Campbell, K.W., Silva, W.J. [2016] "Relative Differences between Nonlinear and Equivalent-Linear 1-D Site Response Analyses," *Earthquake Spectra* 32(3), 1845-1865.
- Knopoff L. [1964] "A matrix method for elastic wave problems. *Bulletin of Seismological Society of America*," 54, 431–438.
- Kramer, S.L., Arduino, P., Sideras, S.S. [2012] "Earthquake Ground Motion Selection," *Washington State Transportation Center*,
<<https://www.wsdot.wa.gov/research/reports/fullreports/791.1.pdf>>
- Ketchum, M., Chang, V., and Shantz, T. [2004] "Influence of Design Ground Motion Level on Highway Bridge Costs," *Pacific Earthquake Engineering Research (PEER) Center, Report No. Lifelines 6D01, University of California, Berkeley, California.*
- Lin, Y. C., Joh, S. H., and Stokoe, K. H. [2014] "Analyst J: Analysis of the UTexas 1 Surface Wave Dataset Using the SASW Methodology," *Geo-Congress 2014 Technical Papers: Geo-Characterization and Modeling for Sustainability. GSP 234. 2014.*
- Liu, W., Stephenson, W. [2004] "Seismic Reponse of Two Specific Sites in the New Madrid Seismic Zone," *Geotechnical Engineering for Transportation Projects (GeoTrans). Los Angeles, California, pp. 1682-1690.*

- Malekmohammadi, M., Pezeshk, S. [2015] “Ground Motion Site Amplification Factors for Sites Located within the Mississippi Embayment with Consideration of Deep Soil Deposits,” *Earthquake Spectra* 31(2), 699-722.
- McGuire, R.K., Silva, W.J., Costantino, C.J. [2001] “Technical Basis for Revision of Regulatory Guidance on Design Ground Motions: Hazard- and Risk- consistent Ground Motion Spectra Guidelines,” NUREG/CR – 6728. <<https://www.nrc.gov/docs/ML0131/ML013100012.pdf>>
- Mento, D.J., Ervin, C.P., McGinnis, L.D. [1986] “Periodic energy release in the New Madrid seismic zone,” *Bulletin of the Seismological Society of America* 76, 1001-1009.
- NEHRP Consultants Joint Venture. [2011] “Selecting and Scaling Earthquake Ground Motions for Performing Response-History Analyses,” NIST GCR 11-917-15.
- Park, C.B., Miller, R.D. and Xia, J. [1999] “Multichannel analysis of surface waves.” *Geophysics* 64(3), 800-808.
- Ramírez-Guzmán, L., Boyd, O., Hartzell, S., Williams, R. [2012], “Seismic velocity model of the central United States (Version 1): Description and simulation of the 18 April 2008 Mt. Carmel, Illinois, Earthquake,” *Bulletin of the Seismological Society of America*, 2622-2645. <<http://pubs.er.usgs.gov/publication/70045157>>.
- Rathje, E.M., Kottke, A.R., Trent, W.L. [2010] “Influence of Input Motion and Site Property Variabilities on Seismic Site Response Analysis,” *Journal of Geotechnical and Geoenvironmental Engineering* 136(4), 607-619.
- Rogers, D. J., Karadeniz, D., Kaibel, C.K. [2007] “Seismic Site Response Modeling for Three Missouri River Highway Bridges,” *Journal of Earthquake Engineering* 11, 400-424.
- Romero, S.M., Rix, G.J. [2001] “Ground Motion Amplification of Soil in the Upper Mississippi Embayment,” National Science Foundation Mid America Center, GIT-CEE/GEO-01-1, Atlanta, Georgia.
- Rosenblad, B., Bailey, J., Csontos, R. and Van Arsdale, R. [2010] “Shear Wave Velocities of Mississippi Embayment Soils from Low Frequency Surface Wave Measurements,” *Soil Dynamics and Earthquake Engineering* 30, 691 – 701.

SESAME, [2004], “Guidelines for the implementation of the H/V spectral ratio technique on ambient vibrations: measurements, processing and interpretation,”
<<http://sesamefp5.obs.ujfgrenoble.fr/Delivrables/Del-D2>>

Stewart, J.P., Kwok, A.O.-L., Hashash, Y.M.A., Matasovic, N., Pyke, R., Wang, Z., Yang, Z. [2008] “Benchmarking of Nonlinear Geotechnical Ground Response Analysis Procedures,” PEER Report 2008/04, Pacific Earthquake Engineering Research Center, University of California, Berkeley, 186 pp.

Thomson, W. T. [1950] “Transmission of elastic waves through a stratified solid medium, Journal of Applied Physics,” 21, 89–93.

Van Arsdale, R.B., TenBrink, R.K. [2000] “Late Cretaceous and Cenozoic Geology of the New Madrid Seismic Zone,” Bulletin of the Seismological Society of America 90, 345–356.

Wang, Z. Zeng, X., Woolery, E., Street, R., Ni, B. [1996] “A Comprehensive Geological and Geotechnical Study on Site Response At Selected Sites in the New Madrid Seismic Zone,” Eleventh World Conference on Earthquake Engineering. Paper No. 1631.

Wathelet, M., Jongmans, D., Ohrnberger, M., Bonnefoy-Claudet, S. [2008], “Array performances for ambient vibrations on a shallow structure and consequences over Vs inversion,” Journal of Seismology 12, 1-19.

WINSEISAB (v5.0.8) [2009]. Computer software. Rancho Cordova, CA: TRC Companies, Inc.

Wood, C., Ellis, T., Teague, D., & Cox, B. [2014] “Analyst I: Comprehensive Analysis of the UTexas1 Surface Wave Dataset, ASCE Geo-Congress 2014: Geo-Characterization and Modeling for Sustainability,” Atlanta, GA, 23-26 February 2014.

Youd, T. L., Idriss, I. M., Andrus, R. D., Arango, I., Castro, G., Christian, J. T., Dobry, R., Finn, W. D. L., Harder, L. F., Hynes, M. E., Ishihara, K., Koester, J. P., Liao, S. S. C., Marcuson, W. F., Martin, G. R., Mitchell, J. K., Moriwaki, Y., Power, M. S., Robertson, P. K., Seed, R. B., Stokoe, K. H. [2001] “Liquefaction resistance of soils: summary report from the 1996 NCEER and 1998 NCEER/NSF workshops on evaluation of liquefaction resistance of soils,” Journal of Geotechnical and Geoenvironmental Engineering 127(10), 817–833.

Zheng, W., Hashash, Y., Petersen, M.M., Whittaker, A.S. [2010] "Site-Specific Response Analysis in the New Madrid Seismic Zone," International Conferences on Recent Advances in Geotechnical Earthquake Engineering and Soil Dynamics. 13 pp.

Zywicki, D.J. [1999] "Advanced signal processing methods applied to engineering analysis of seismic surface waves," Ph.D. Dissertation, School of Civil and Environmental Engineering, Georgia Institute of Technology, Atlanta, GA.